Applied Catalysis B: Environmental 184 (2016) 201–207

Contents lists available at ScienceDirect

Applied Catalysis B: Environmental

journal homepage: www.elsevier.com/locate/apcatb

Kinetics of methylene blue (MB) photocatalyzed reduction and dark regeneration in a colorimetric oxygen sensor

David Ollis[a,*], Andrew Mills[b], Katherine Lawrie[b]

[a] Chemical and Biomolecular Engineering, North Carolina State University, Raleigh, NC 27695-7905, USA
[b] School of Chemistry and Chemical Engineering Queens University Belfast, Stranmillis Road, Belfast BT9 5AG, UK

ARTICLE INFO

Article history:
Received 27 March 2015
Received in revised form 23 October 2015
Accepted 10 November 2015
Available online 30 November 2015

Keywords:
Oxygen sensor
Photocatalyst
Methylene blue
Kinetic model

ABSTRACT

Performance data for a dye based, regenerable oxygen sensor (Mills and Lawrie [1], Mills et al. [2]) are analyzed to develop useful kinetic models for sensor photoactivation (dye reduction) and dark, oxygen detection (dye oxidation). The titania loaded, thin film sensor exhibits an apparent first order photoactivation of the dye, which we demonstrate (Section 3.2 and Fig. 4) is due to a kinetic disguise of a zero order photoreaction occurring through a non-uniformly illuminated sensor film. The observed zero order, slow recovery due to dye oxidation by dioxygen (O_2 detection) appears best rationalized by a model assuming a near O_2-impermeable skin developing on the sensor surface as solvent is evaporatively removed following sensor film casting and curing.

1. Introduction

Recent work by Mills and co-workers [1,2] has demonstrated use of the dye methylene blue (MB) as a colorimetric indicator for molecular oxygen presence via the reactions shown in Fig. 1 [1]. These reactions involved photocatalyzed dye reduction (sensor activation) followed by oxygen detection via the dark re-oxidation of the reduced dye. While photoreaction occurred on a time scale of seconds to minutes (fast), the dark re-oxidation required 0.5–5 days, decreasing with increased level of platinization of the rutile TiO_2 dispersed in a (sulfonated polystyrene)/glycerol film [1].

To improve sensor performance, it is useful to establish quantitative models of both reduction and oxidation processes in order to validate/test assumed rate determining steps of each process, and to allow for the possibility of photocolorimetric sensor optimization.

2. Experimental

All data analyzed in the present paper is taken from earlier papers by Mills and Lawrie [1] and Mills et al. [2]. The photoactive film phase of the oxygen sensor was composed of dye methylene blue (MB), titanium dioxide (TiO_2), glycerol, and sulfonated polystyrene (SPS); its synthesis and characterization are described in [1] and [2], and summarized below:

2.1. Oxygen sensor film preparation and compositions

2.1.1. Film sPS/Pt-TiO (1)

Polystyrene (PS) (MW_{ave} = 250,000) sulfonated to 30 wt%. Then 0.25 g sulfonated PS dissolved in 2 g ethanol, added 0.25 g glycerol and 0.1 g Pt (0.38 wt%)/TiO_2. Added 2.5 mg methylene blue (MB), cast on plastic (polypropylene) film, used K-bar to thin film to yield a dry ink of 4–5 μm thickness. Final film was MB/SPS/Pt-TiO_2/glycerol in weight ratio of 1/100/40/100.

2.1.2. Film sPS/TiO_2 (2)

Polystyrene (PS) sullfonated to 10 wt%. Then 0.25 g SPS dissolved in 2 g acetone, added 0.25 g glycerol, and 0.1 g TiO_2 (rutile), mixed and sonicated, added 2.5 mg MB. Final film was MB/SPS/TiO_2/glycerol in weight ratio 1/100/40/100, cast and thinned with K-bar to yield dry ink film of 4–5 μm thickness.

3. Results and discussion

3.1. Photoreduction kinetic data (sensor activation)

The sensor process of Fig. 1 is attractive because the initial sensor photoactivation requires only about 1 min using a 4.5 mW/cm^2 UVA (365 nm) lamp as shown in Fig. 2a and b for sulfonated polystyrene/glycerol films cast from ethanol solutions and includ-

* Corresponding author. Fax: +1 919 515 3465.
E-mail address: ollis@ncsu.edu (D. Ollis).

http://dx.doi.org/10.1016/j.apcatb.2015.11.011
0926-3373/

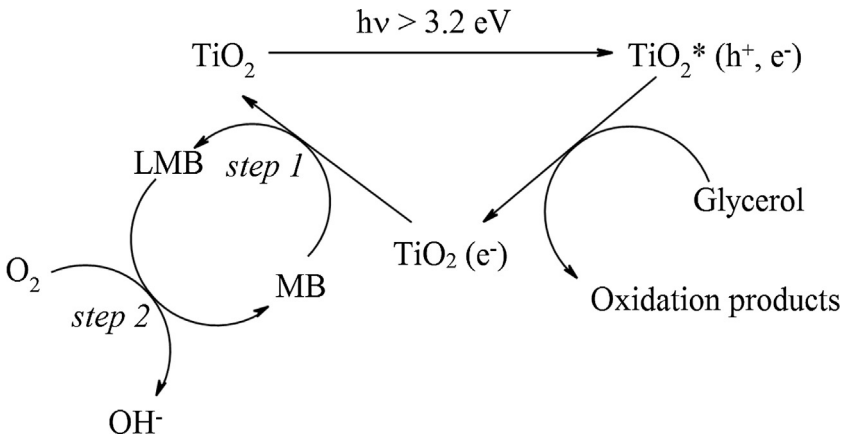

Fig. 1. Mechanism of UV light driven reduction of methylene blue (photoactivation step 1) and its subsequent re-oxidation by ambient air (if present) (dark step 2) [1]. (Reprinted by permission of Elsevier).

ing a platinized photocatalyst, Pt (0.38 wt%)/TiO_2 (Fig. 2a) or cast from acetone solutions and incorporating TiO_2 (Fig. 2b). The kinetics of the rapid photoactivation process appear to be predominantly first order for both sensors, as seen from the linearity of semilog plots in Fig. 3a and b.

Mills and Lawrie [1] platinized TiO_2 photocatalyst was cast in a sulfonated polystyrene film containing a sacrificial agent, glycerol [1]. Application via a doctor blade produced a dried MB/(Pt/TiO_2)/SPS/glycerol membrane film cast from an ethanol solution containing 0.25 g SPS, 0.25 g glycerol, 0.1 g [Pt (0.38 wt%)/TiO_2] and 0.0025 g MB. Assuming for convenience a dried film density of 1 g/cm^3 and measured thickness 5 μm, the TiO_2 content of a 1 cm^2 film is

$$\text{TiO}_2\text{loading} = (0.1\,\text{gTiO}_2/0.6\,\text{gfilm}) \times 5 \times 10^{-4}\,\text{cm} \times 1\,\text{g/cm}^3 = 8.3 \times 10^{-5}\,\text{g/cm}^2.$$

A similar thickness and TiO_2 loading was used in [2].

The light traversing the TiO_2 layer is subject to both absorption and to scattering. The relative contributions to removal of light from the original light path were determined by Cabrera et al. [3] to produce extinction ($ß$) and absorption (μ) coefficients, for Aldrich TiO_2 in aqueous suspensions with values at 365 nm of $ß = 3.8 \times 10^4$ cm^2/g and $\mu = 0.25 \times 10^4$ cm^2/g. Thus, these particles are about 15 times more likely to scatter UVA light than to absorb it.

The apparent optical density due to absorption in a non-scattering medium is

$$\text{OD}_{\text{app}} = \mu\,[\text{TiO}_2] = 0.25 \times 10^4 \text{cm}^2/\text{g} \times 8.3 \times 10^{-5}\text{g TiO}_2/\text{cm}^2 = 0.21$$

In consequence, the transmittance T is given by

$$T = 10^{-\text{ODapp}} = 0.61, \text{ so 39\% of the light is absorbed in straight passage through a 5μm film} \quad (2)$$

However, the heavy scattering of light within the sensor film lengthens the average photon path considerably, and if the actual path of the repeatedly scattered beam were 2, 3, or 4 times the apparent film thickness of 5 μm, the effective optical density would become 0.42, 0.63, and 0.84, leading to calculated transmittances of 38% ($10^{-0.42}$), 23% ($10^{-0.63}$), or 14%, ($10^{-0.84}$), respectively. Thus, a steep gradient of irradiance would exist within the film, a condition we have previously shown to give disguised kinetic orders of reaction for both stearic acid multilayers [4], and submonolayers and multilayers of organic dyes dispersed throughout a porous TiO_2 layer [6].

Thus, the TiO_2 in the mixed composition thin film loaded with 8.3×10^{-5} g TiO_2/cm^2 absorbs or scatters nearly all incident UVA irradiation, and therefore a strong illumination gradient, exponential in the simplest analysis, exists within the thin film. Given that the local reaction rate constant depends upon local intensity, a spatial gradient in the local rate of photoreduction of MB is also present.

3.2. Photoreduction kinetic model

The relatively rapid dye reduction appears to be globally first order in MB (dye) concentration (Fig. 2b). However, for this thin film circumstance where light absorption is complete, we have previously shown that due to the spatial variation of intensity, and thus local photocatalyzed rate constant, a zero order photocatalyzed reaction could exhibit a disguised first order global behavior [4,6].

Such a disguise must be present here, as the TiO_2 scattering and absorbance is sufficient to capture all arriving photons. (The sulfonated polystyrene has negligible UVA absorbance [5].)

We demonstrate this notion here by approximating the continuous exponential decline of intensity within the thin film by a discrete model of five parallel layers, each of which has a rate constant equal to one half that of the preceding layer, thus approximating an exponential decline in irradiance with depth into the film, and thus a corresponding decline in local rate constant, assuming k is proportional to the local layer irradiance. Thus the zero order local rate will have an activity in succeeding layers of k, $k/2$, $k/4$, $k/8$ and $k/16$.

Assuming that the mass M_i vs time function of unconverted dye in each layer $i = 1,...,5$ is given by the zero order equation, then

$$M_i = M - k_i t \quad (3)$$

where M = initial dye in each layer.

The total unreacted dye in the film, $M_T(t)$, changes with time according to the sum of all layers:

$$M_T(t) = \sum M_i(t) = \sum (M - k_i t) \quad (4)$$

Each layer is exhausted of dye at time satisfying $M_i = 0 = M - k_i\, t_i$, thus at $t_i = M/k_i$.

Consider a five layer approximation. At $t = 0$, each layer has a mass M of dye, and the total initial mass of dye in the film is 5 M. At

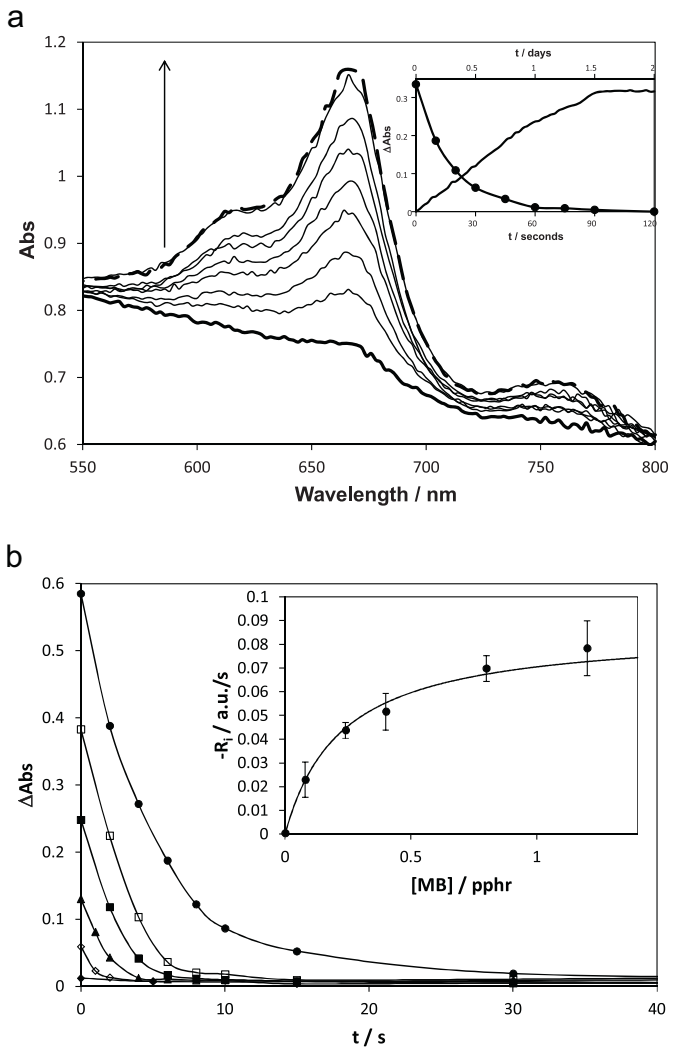

Fig. 2. (a) Plot of UV–vis spectra of a typical Pt-TiO_2/MB/glycerol/SPS oxygen-indicating film before (bold, dashed) and after (bold) the UVA light activation (60 s of UVA/4.5 mW cm^{-2}) step, followed by subsequent spectra taken at 3, 6, 9, 12, 18, 24 and 36 h after photoactivation. The insert plot illustrates the change in absorbance, ΔAbs, at λ_{max} (665 nm) upon 120 s UVA activation at 4.5 mW cm^{-2} (left and lower *x*-axis, circles) and subsequent exposure to ambient air, after photoactivation (left and upper x-axis). [1] (Reprinted by permission of Elsevier). (b) Plot of ΔAbs vs. the time of irradiation for TiO_2/MB/glycerol/SPS indicator films containing different pphr of MB. The covering range: 0 (♦), 0.08 (◊), 0.24 (▲), 0.4 (■), 0.8 (□) and 1.2 (●) pph of MB. The insert diagram is a subsequent plot of the data in the form of initial rate, ri vs. [MB], along with associated error bars. Data from Mills, Hazafy and Lawrie [2]. (Reprinted by permission of Elsivier).

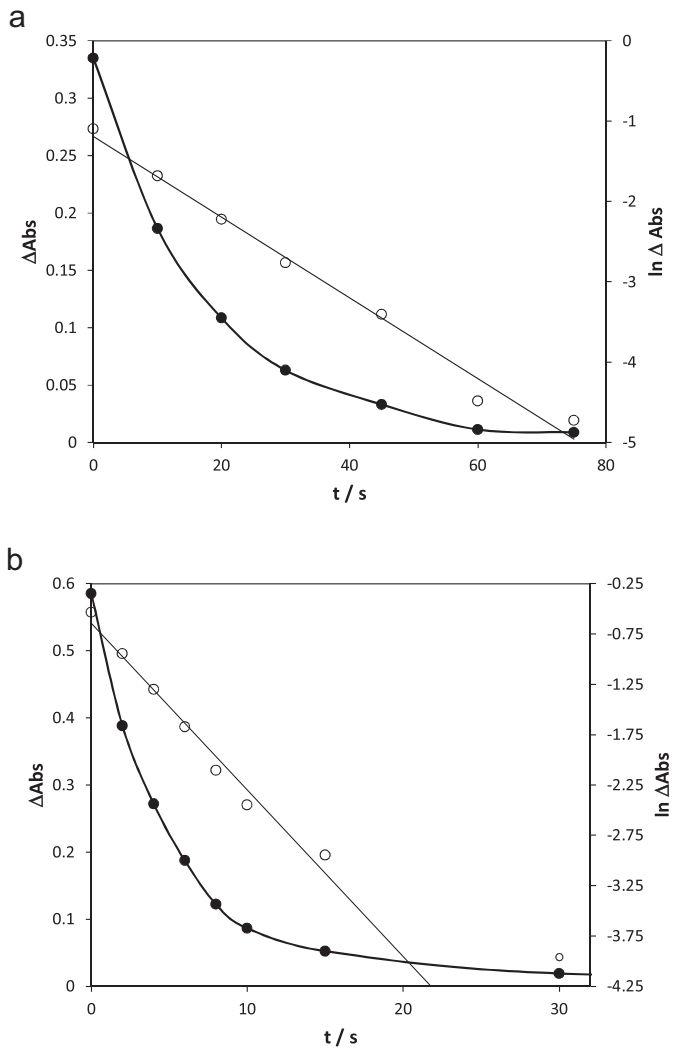

Fig. 3. (a) Photoactivation data of Fig. 2a (●, left axis), and semilog plot of this data (◯, right axis). (b) Photoactivation data for [MB] initial = 1.2 pph (top curve) in Fig. 2b (●, left axis), and semilog plot of this data (◯, right axis).

$t = M/k$, the first layer is exhausted, and the mass of each remaining layers is given below:

$$M_1 = 0$$

$$M_2 = M - \left(k/2\right)\left(M/k\right) = M/2$$

$$M_3 = M - \left(k/4\right)\left(M/k\right) = 3M/4$$

$$M_4 = M - \left(k/8\right)\left(M/k\right) = 7M/8$$

$$M_5 = M - \left(k/16\right)\left(M/k\right) = 15M/16$$

Thus, at $t = M/k$, the total remaining dye, $M_T(t)$ is

$$M_T\left(t = M/k\right) = M\left(1/2 + 3/4 + 7/8 + 15/16\right) = 3.06M$$

Similar calculations for M_T at the exhaustion of each deeper layer produce M_T

$$\left(t = 2M/k\right) = 2.13M,\ M_T\left(t = 4M/k\right) = 1.25M,$$

$$\text{and} M_T\left(t = 8M/k\right) = 0.5M.$$

A semilogarithm plot of these data as ln M_T vs. time, *t*, appears in Fig. 4, and is seen to provide a good "first order" fit, i.e., a kinetic disguise as we earlier noted, arising because of the spatial variation of k with depth into the photocatalyst film [4,6].

Further evidence supporting our assumption of zero order local (intrinsic) rate is found from a plot of initial rate vs. initial dye concentration, which was fitted [2] earlier to the Langmuir–Hinshelwood (LH) form,

$$R = k_{LH}\left[\frac{K\,[\mathrm{MB}]}{1 + K\,[\mathrm{MB}]}\right] \quad (5)$$

with $K = 4.48$ pp h^{-1} and $k_{LH} = 0.09$ au/s. The data in Fig. 2a were acquired at concentration MB = 1 pp h (part per hundred resin [sulfonated polystyrene]), thus the MB concentration dependent term which represents fractional catalyst surface coverage has an initial value of K[MB]/(1 + K [MB]) = 4/5 = 0.8. The catalyst surface is initially nearly covered, and an approximately zero order, initial

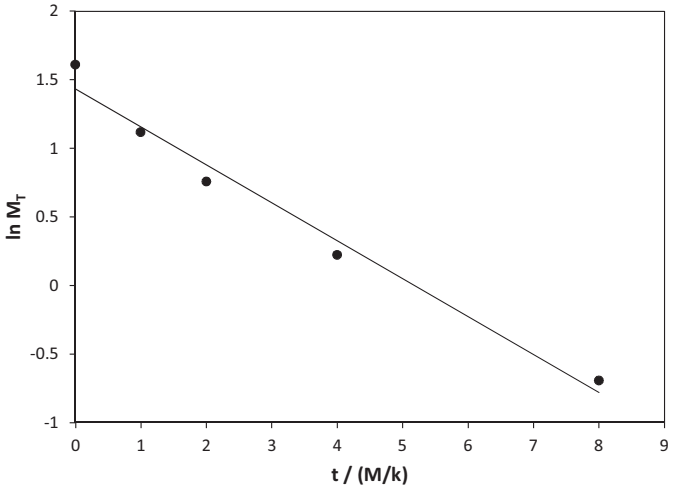

Fig. 4. Model: semilog plot of calculated total remaining dye mass, M_T, vs. time, t, showing apparent first order behavior. [6] (Reprinted by permission of Elsevier).

local rate would be expected. Our discrete layer analysis above indicates that the apparent initial rate, assessed over $t = M/k$, equals $-k$ $(1 + ½ + ¼ + 1/8 + 1/16 \ldots) = -2k$.

Thus,

$$\text{apparentrate} = -k_{LH}\left(K\,[\text{MB}]/1 + K\,[\text{MB}]\right) = -0.8k_{LH} \quad ,$$

and the zero order initial rate has the value of

$$\text{rate} = -2k = -0.8k_{LH} \quad ,$$

hence,

$$k = \left(0.8/2\right) x0.09\,\left(\text{au/s}\right) = 0.036\,\left(\text{au/s}\right)$$

At much lower dye concentrations, a different kinetic behavior is predicted. For an initial dye concentration MB « $1/K = 0.25$ pp h, the reaction rate should be first order locally, and for complete light absorption, the total film would likely exhibit a similar kinetic disguise of a higher apparent order = 2, as we have previously demonstrated for other low coverage dyes immobilized in TiO_2 films [6].

3.3. Influence of photocatalyst loading on photoreduction

The conversion of MB to its reduced form, leucomethylene blue (LMB), vs time due to UVA photoreduction as a function of [TiO_2] loading in the film is shown in Fig. 5a [2]. The initial rates calculated from these data are plotted vs photocatalyst loading in Fig. 5b, showing that a linear relation exists, confirming that the reduction is a catalyzed reaction, as noted earlier [2].

To compare the observed rate to the model, we need to assume a factor for the true vs. apparent photon path length. For the sake of example, we assume a factor of three, corresponding to a predicted transmittance of 23% at the maximum loading used of 8.3×10^{-5} g/cm^2. For films which are of 100, 80, 60, 40, and 20% of this maximum value loading, we calculated transmittances of 23, 31, 42, 56, and 75%, leading to fraction of absorbed light values $(1 - T)$ of 0.77, 0.69, 0.58, 0.44, and 0.25, respectively. These calculated values (circles) are plotted along with the experimental data contained in Fig. 5b (squares) and c. The correspondence indicates the plausibility of the scattering path assumed.

3.4. Dark oxidation (sensor operation)

The dye regeneration is a dark reaction (Fig. 1), and exhibits an apparent zero order behavior (Fig. 2a, inset) for one day, reaching

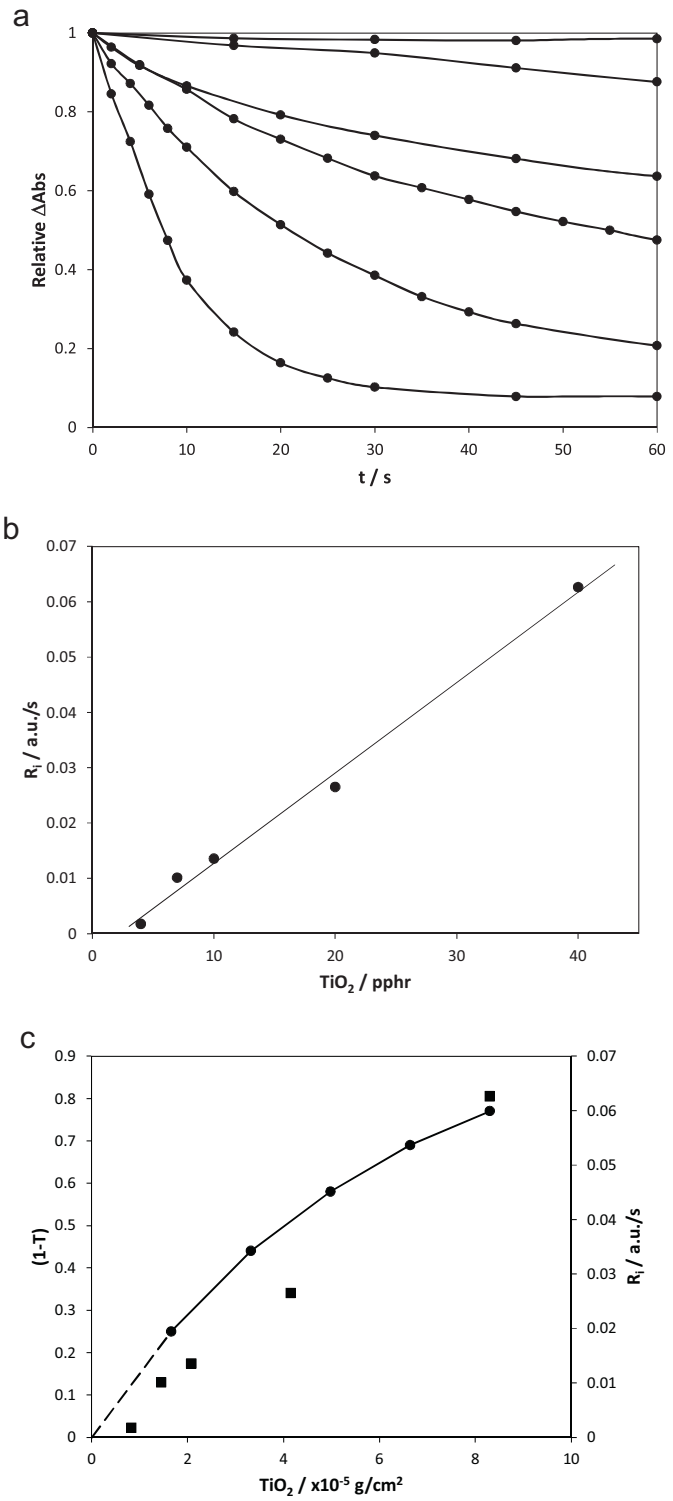

Fig. 5. (a) Relative change in absorbance, Abs vs. time of UVA photreduction of a MB/SPS/TiO_2/glycerol film as a function of TiO_2 concentration in the film. The data lines refer to 0, 4, 7, 10, 20, and 40 pph (top to bottom) of TiO_2 used in the O_2 indicator formulation. [2]. (Reprinted by permission of Elsevier). (b) Measured initial rate vs. TiO_2 photocatalyst loading in film, showing that observed photoactivation is a catalyzed reaction (zero rate with no catalyst). (c) Plot of the calculated fraction of photons absorbed for a non-scattering film (●) and measured initial rate (■) vs. photocatalyst loadings of (a) and (b).

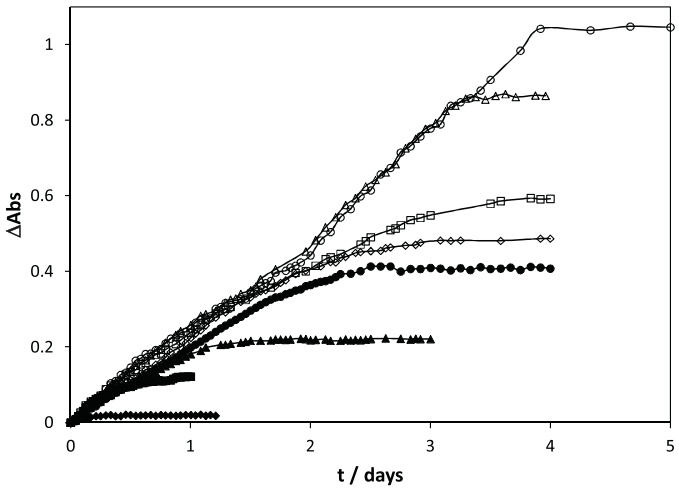

Fig. 6. Dark regeneration: Change in absorbance at 665 nm for oxygen indicators cast with K-bars 1–8, with measured average thicknesses of 0.35 (filled diamonds), 1.00 (filled squares), 2.70 (filled triangles), 4.00 (filled circles), 5.95 (open diamonds), 7.85 (open squares), 9.00 (open triangles) and 13.00 μm (open circles). [1]. (Reprinted by permission of Elsivier).

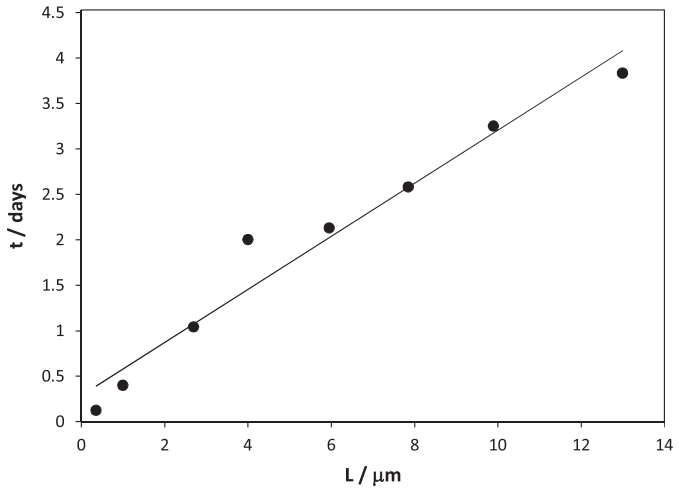

Fig. 7. Complete film regeneration time vs layer thickness. Data represent the intersection of initial regeneration rate with final, horizontal asymptote (complete regeneration) for Fig. 6 data.

full regeneration at 1.5 days. The dark step recovery involves the reaction

$$O_2 + DYE_{red} \rightarrow DYE^{+}{}_{ox} + 2OH \quad (6)$$

3.5. Kinetic data of dye dark regeneration

Mills and Lawrie [1] examined the variation of slow recovery time with film thickness, with results shown in Fig. 6. For each film we estimate the time to complete regeneration by noting the time at which the initial slope intersects the eventual horizontal asymptote for each experiment, which signals complete film regeneration. A plot of such completion times vs. layer thickness, *L*, is linear, as seen in Fig. 7. The zero order rate (and rate constant) is calculated from film exhaustion time, e.g., a 13 μm layer is converted in 4 days, thus the rate constant is 3.25 μm/day (or ca. 3×10^{-6} a.u./s from the data in Fig. 6) for all films shown, since all appear to have similar slopes.

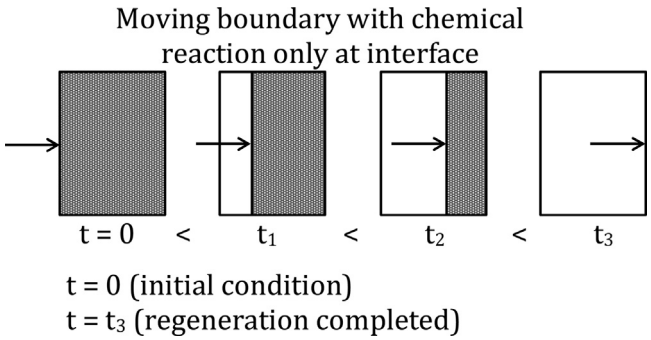

Fig. 8. Example of progression of a moving boundary with time for a zero order interfacial reaction. Assumed constant rate of interfacial reaction leads to zero order reaction rate and a regeneration time scaling with film thickness.

3.6. Kinetic analysis of dark dye regeneration: mechanistic considerations

We now consider various mechanisms which could lead to an apparent zero order regeneration rate.

3.6.1. Moving boundary hypothesis

The linear scaling of regeneration completion time with film thickness (Fig. 7) suggests a rate limiting, zero order moving boundary problem, as illustrated in Fig. 8. The regeneration reaction, Eq. (6), consumes oxygen and generates water, and occurs only at the moving boundary between the reduced dye and regenerated (oxidized) dye region. The regenerated dye is reversibly immobilized on both the SPS polymer and the TiO_2 photocatalyst through ionic interactions with the negative sulfonate group of the polymer and the anionic groups of the TiO_2 surface, for example.

A zero order dark reaction is currently unknown. One potential scenario which could result in a propagating reaction front is an oxygen utilizing, Pt catalyzed oxidation of glycerol and/or polystyrene, producing lower molecular weight products, and thereby substantially reducing the viscosity, hence increasing the permeability of the original SPS/glycerol dried film. Mills and coworkers earlier noted that the regeneration reaction proceeds far faster in films cast in water based ink than in the glycerol/sulfonated polystyrene phases cast from ethanol or acetone inks [1,2]. However, upon repeated cycling of a later film composition (TiO_2/tartrate/MB) [7], the regenerated resin appears to have similar photoactivation and subsequent recovery dynamics upon repeated cycling, a repeatable recovery behavior inconsistent with the assumed phase-like change posited to explain a one-time, moving boundary behavior. If however, the re-oxidation of the dye somehow restored the entire film to its original, more viscous or solid state, then such a mechanism could rationalize the observed behavior. This hypothesis seems unlikely.

3.6.2. Mobile dye adsorbed strongly on Pt hypothesis

A second mechanism which could exhibit zero order regeneration kinetics in terms of dye concentration is shown below:

$$O_2\,(gas) \Leftrightarrow O_2(film) \qquad (rapid) \quad (7)$$

If the coverage of reduced Dye(red) on Pt/TiO_2 remains constant over the conversion period via replenishment by mobile dye from the film SPS/glycerol phase, a zero order recovery is expected, in agreement with experiment (Fig. 6).

k_2 (Pt)

$$O_2\,(flim) + Dye\,(red) \rightarrow Dye\,(ox) + 2OH^{-}(slow) \quad (8)$$

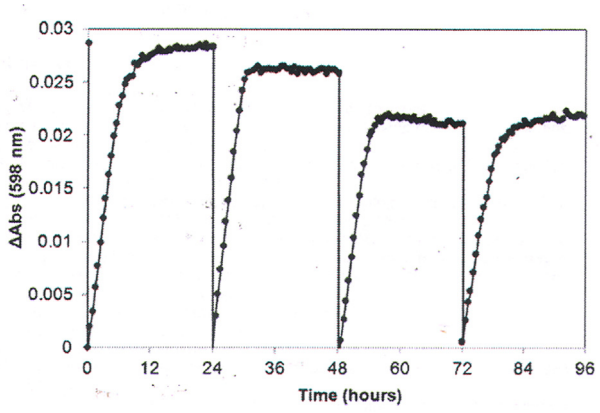

Fig. 9. Absorbance (598 nm) of MB/tartrate film during cycling between oxidation and light induced reduction (UVA) showing repeatable zero order regeneration. [7] (Reprinted by permission of Elsevier).

The ring sulfur of thiophene is known to bind strongly to platinum [8], hence we could expect the ring sulfur of leucomethylene blue (reduced MB) to adsorb on platinum to saturation coverage at room temperature. The uncharged leucomethylene blue would be mobile in the bulk SPS/glycerol film and not expected to bind strongly to sulfonate groups, in contrast to the oxidized form, MB. This zero order reaction possibility does not explain Fig. 7, however, as the above mechanism predicts a recovery time independent of film thickness, in contrast to the data of Figs. 6 and 7.

3.6.3. Glassy SPS phase hypothesis

A third possibility we believe to be most probable. The original TiO_2/sulfonated polystyrene/glycerol/dye film of Mills and co-workers [1,2] were cast using ethanol [1] or acetone [2] as a solvent for SPS and glycerol. A zero order regeneration is possible if a "skin" of constant thickness, e.g., resistance to oxygen/water diffusion, is formed at the air-film interface as the solvent evaporates (Fig. 10). The driving force for film formation comes from two potential mechanisms: preferred adsorption of polystyrene at the air–solid interface and glycerol–polystyrene phase separation. We speculate on these two potential driving forces.

First, the predominantly hydrophobic sulfonated polystyrene is expected to prefer the air–solid interface vs. the more hydrophilic glycerol. During evaporative removal of solvent as part of the film casting procedure, the increasingly incompatible SPS and glycerol would exhibit phase separation, with some SPS moving to the air–film interface.

Support for the glass phase formation hypothesis is seen from the following literature:

(1) Polystyrene–glycerol blends are incompatible: non-ionic (native) polystyrene (PS) is insoluble in "glycerol at room temperature. ...In addition, PS film surfaces were not swollen by ... glycerol" over a 3 min contact with a thin film ." [9]
(2) Glycerol is only somewhat soluble in sulfonated polystyrene: PS sulfonation increases the solubility of glycerol only somewhat, allowing its use as a plasticizer for sPS. However, for the 1:1 weight ratio of glycerol and sulfonated polystyrene used in studies [1] and [2] analyzed here, a phase separation is still expected upon solvent removal. For example Weiss et al. [10] reported that glycerol/2.9% sulfonated polystyrene mixtures exhibited phase separation above 8% glycerol. Their separated polystyrene phase exhibited glass formation with a glass transition temperature, T_g, only slightly below that of the pure polystyrene (about 105 °C) [10].
(3) Addition of oxide nanoparticles does not substantially change polymer glass formation. The addition of 20 wt% of amine-functionalized silica nanoparticles caused only a 9 °C increase in T_g of sulfonated polystyrene,and did not prevent glass formation [11].

The colorimetric sensor film of Ref. [1] had a composition of MB/SPS/Pt-TiO_2/glycerol in weight ratio of 1/100/40/100, all originally dissolved/dispersed in ethanol. Thus the polymer blend is 50% SPS and 50% glycerol, with an added 20% of TiO_2 particles. We conclude that neither glycerol addition nor addition of small particles, like SiO_2 or TiO_2, to sulfonated polystyrene prevents formation of polystyrene-rich glassy phases with glass transition temperatures in the range of 90–115 °C. Thus, this literature supports our proposal that a diffusion resistant skin, rich in glassy sulfonated polystyrene forms upon solvent removal, and may be the cause of the ensuing slow regeneration times shown Figs. 2a (insert) and 6.

This skin would be a major diffusion resistance to both oxygen and solvent, and a zero order regeneration reaction kinetics could be expected, since the impermeable outer skin of approximately constant thickness would provide the dominant oxygen (and/or water) diffusion uptake resistance.

A similar, repeatable behavior occurs with tartrate films (Fig. 9b).

A model for oxygen diffusion through the dense "skin" would be simply

$$D_{O2} dC(O_2)/dx = 0,$$

with boundary conditions of $C(O_2)^* = 0.21$ atm at the air–film interface, and $C(O_2) = 0$ (approximately) at the skin–film interface (Fig. 9b). This model predicts a constant flux once the skin is formed, and a flux which varies linearly with oxygen pressure, as reported in [1,2]. In such a case, the thicker the ink films, and so the greater the number of molecules of LMB that need to be re-oxidized by O_2, the longer the predicted time for the film to fully recover its original color, a behavior consistent with the data in Figs. 6 and 7.

4. Other related work

A later paper by Lawrie et al. [7] explored photoactivation and dark, oxygen regeneration of O_2 sensors based upon MB/TiO_2/tartaric acid films. With evaporative removal of solvent water from the MB/TiO_2/tartaric printed ink, we may suppose formation of a film of tartaric acid crystals. As crystals are virtually impermeable to gases, we again assume that a gas diffusion barrier is formed, with a gas-liquid surface drying to produce a crystalline "skin". Such a skin formed in the film casting step could subsequently produce a repeatable, zero order oxidative regeneration step as seen in Figs. 9 and 10.

A similar, slow, repeatable regeneration, showing a clear zero order regime, albeit with an initial positive order region, was reported by Galagan and Su [12] for TiO_2/MB/acrylate sensor (Fig. 11) for a sensor film thickness of 100 μm. These authors attributed the slow kinetics to small oxygen diffusivities within their presumably glassy acrylate made by mixing monomers 2 hydroxyethyl methacrylate and tricyclodecane diethanol diacrylate (TCDDA). Subsequent photopolymerization would produce a glassy phase with transition temperature between that of pure poly(HEM) (50 °C) and poly(TCDDA)(186 °C), with an expected long regeneration time, at ambient temperature, consistent with the 8 days reported by them [12].

Vu and Won [13] formed a MB based oxygen indicator by entrapping a dye/TiO_2/glycerol/zein combination within an alginate coating. Alginate does not form a glassy or crystalline phase, and the more open alginate coating (thickness unknown) retained

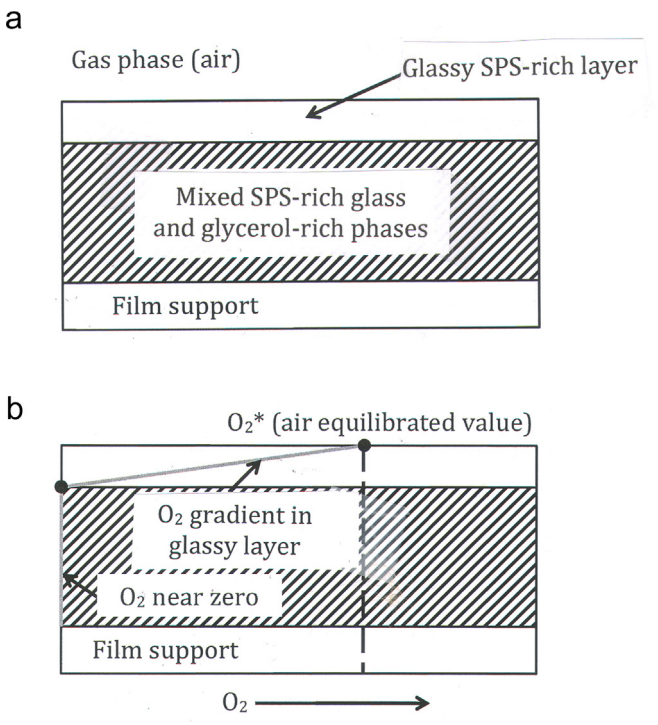

Fig. 10. (a) Example of mixed film separated into a glassy outer SPS-rich layer and an inner glycerol-rich layer. Glassy phase provides strong diffusional resistance for oxygen transport, leading to zero order reaction rate and a regeneration time scaling with film thickness. (b) Example dissolved oxygen profile in sensor film of Fig. 9a.

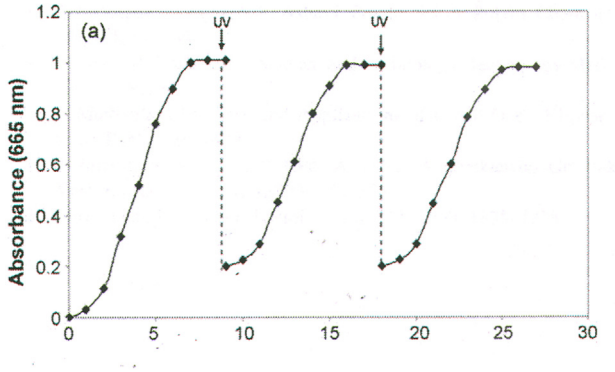

Fig. 11. Absorbance (665 nm) of MB/acrylate film during cycling between oxidation and light induced reduction (UVB) showing zero order regime during reduction [12]. (Reprinted by permission of Elsevier).

at 24 h. more that 80% of the initial dye loading, due, the authors suggest, to the polyanionic alginate binding of any diffusing cationic MB dye. The regeneration time was only 4 h. This faster regeneration time is consistent with our argument above regarding the slower regeneration of sensor films containing components capable of forming glassy phases.

Similarly, aqueous hydroxyethycellulose (HEC)-based solutions produced a hygroscopic film [14]. Pure HEC contains 5–10% water at ambient temperature equilibration with 30–60% relative humidity air, and such a swellable material is not expected to crystallize or form a glass, but rather form a more oxygen permeable film and provide the much faster regeneration time noted in Table 1.

The research into photochemical oxygen sensors has included work by Mills and co-workers [1,2,7,14,15], Vu and Won [13], and Galagan and Su [12]. A comparison of the sensor film compositions, dyes, and reduction and regeneration (oxidation) times is summarized in Table 1 above. The sensor recovery times are often oxygen dependent [7,14,15], indicating a dependence upon oxygen diffusion and/or reaction. Mills and Lawrie [1] proposed that their SPS/glycerol MB sensors were regeneration controlled by slow oxidation "in the low dielectric polymer encapsulation medium", rather than by oxygen diffusion, but the observation of zero-order kinetics for reaction (6) and dependence of regeneration time on film thickness coupled with the above model suggests this is not the case. The relative dependence of regeneration on diffusion vs reaction needs further study, as the other papers in Table 1 do not demonstrate which processes are dominant.

Table 1
Comparison of photocatalytic oxygen dye sensors.

Ref.	Dye	Other Components	*t* (red)	*t* (regen)
[1]	MB	(Pt/TiO_2)/SPS/glycerol	<90 s	1.5 days
[2]	MB	TiO_2/SPS/glycerol	<60 s	5 days
[7]	MB	TiO_2/tartrate	3 min	12 h
[12]	MB	TiO2/polyacrylates	–	8 days
[13]	Thionine	TiO_2/zein/alginate/glycerol	5 min	4 h
[14]	MB	SnO_2/hydroxyethyl cellulose/glycerol	100 s	5 min
[15]	MB	TiO_2/LDPE/threitol	<90 s	2.5 days

5. Other organic dyes

Other dye candidates could be considered as well. Many different dye types are photoreduced by TiO_2, to yield forms that are O_2 sensitive, i.e. once photoreduced, their original color can be recovered upon exposure to O_2. All the thiazines do it (including methylene blue and thionine), as do oxazones (such as resorufin), triphenyl methane dyes (such as Acid Blue 9), and anthraquinone dyes (such as Acid Blue 129). We know those dyes in brackets work well, but none have the very substantial molar absorbtivity, ca. 74,000 M^{-1} cm^{-1} and stability (required for repeated use) of methylene blue.

6. Conclusion

Oxygen sensors based on photocatalyst–polymer–sacrificial agent combinations are attractive for their ease of fabrication and use, but a full kinetic model for these systems is shown to require consideration of light profiles in these thin layer sensors, as well as the phase behavior of the regenerated final films.

References

[1] A. Mills, K. Lawrie, Sens. Actuators B Chem. 157 (2011) 600–605.
[2] A. Mills, D. Hazafy, K. Lawrie, Catal. Today 161 (2011) 59–63.
[3] M. Cabrera, O.M. Alfano, A. Cassano, J. Phys. Chem 100 (1996) 20043–20051.4.
[4] D. Ollis, Appl. Catal. B Environ. 99 (2010) 478–484.
[5] A. Marletta, K. Campos, S. Nogueira, A. Andrade, N. Neto, R. Silva, J. Non-Cryst. Solids 356 (2010) 2414–2416.
[6] D. Ollis, Appl. Catal. B Environ. 165 (2015) 111–116.
[7] K. Lawrie, A. Mills, D. Hazafy, Sens. Actuators B Chem. 176 (2013) 1154.
[8] H. Wang, E. Iglesia, ChemCatChem 3 (2011) 1166–1175.
[9] B. Zuo, et al., Macromolecles 46 (2013) 1875–1882.
[10] R. Weiss, R.J. Fitzgerald, D. Kim, Macromolecules 24 (1991) 1064–1070.
[11] S. Kim, et al., Nanoscale 7 (2015) 8864.
[12] Y. Galagan, W.-F. Su, J. Photochem. Photobio. A Chem. 195 (2008) 378–383.
[13] A. Vu, K. Won, Food Chem. 140 (2013) 52.
[14] A. Mills, D. Hazafy, Sens. Actuators B Chem. 136 (2009) 344.
[15] A. Mills, et al., Analyst 7 (2012) 106.